The impact of the mixing properties within the Antarctic stratospheric vortex on ozone loss in spring

JOURNAL OF GEOPHYSICAL RESEARCH, VOL. 106, NO. D3, PAGES 3203-3211, FEBRUARY 16, 2001

The impact of the mixing properties within the Antarctic stratospheric vortex on ozone loss in spring

Adrian M. Lee,[1] Howard K. Roscoe,[2] Anna E. Jones,[2] Peter H. Haynes,[3] Emily F. Shuckburgh,[3] Martin W. Morrey,[4] and Hugh C. Pumphrey[4]

Abstract. Calculations of equivalent length from an artificial advected tracer provide new insight into the isentropic transport processes occurring within the Antarctic stratospheric vortex. These calculations show two distinct regions of approximately equal area: a strongly mixed vortex core and a broad ring of weakly mixed air extending out to the vortex boundary. This broad ring of vortex air remains isolated from the core between late winter and midspring. Satellite measurements of stratospheric H_2O confirm that the isolation lasts until at least mid-October. A three-dimensional chemical transport model simulation of the Antarctic ozone hole quantifies the ozone loss within this ring and demonstrates its isolation. In contrast to the vortex core, ozone loss in the weakly mixed broad ring is not complete. The reasons are twofold. First, warmer temperatures in the broad ring prevent continuous polar stratospheric cloud (PSC) formation and the associated chemical processing (i.e., the conversion of unreactive chlorine into reactive forms). Second, the isolation prevents ozone-rich air from the broad ring mixing with chemically processed air from the vortex core. If the stratosphere continues to cool, this will lead to increased PSC formation and more complete chemical processing in the broad ring. Despite the expected decline in halocarbons, sensitivity studies suggest that this mechanism will lead to enhanced ozone loss in the weakly mixed region, delaying the future recovery of the ozone hole.

1. Introduction

The Antarctic ozone hole [*Farman et al.*, 1985] is now a well-established feature of the Antarctic stratosphere in spring. It is confined within a vortex of stratospheric winds and remains largely isolated from the middle latitudes. The persistent mean meridional circulation brings unreactive chlorine compounds, which originate from man-made halocarbons, from the upper stratosphere into the polar vortex and to altitudes where polar stratospheric clouds (PSCs) form. Reactions on these cloud particles convert the unreactive chlorine compounds into reactive forms which then catalyze ozone loss in sunlight [*World Meteorological Organization*, 1989]. In the vortex core, PSCs are ubiquitous [*McCormick*, 1983; *Cacciani et al.*, 1997], so that ozone loss is determined by the supply of unreactive chlorine. We expect ozone loss in the vortex core to diminish during the next 50 years, as amounts of halocarbons decline due to the provisions made in the Montreal Protocol and subsequent revisions [*Pyle et al.*, 1996].

With the rapid polar ozone loss processes initiated by sunlight, the ozone hole develops from the vortex-edge region inward to the core. The poleward propagation of this ozone loss in the presence of reactive chlorine is limited by the poleward retreat of the terminator (the boundary which delineates polar night), by planetary waves exposing deeper vortex air to sunlight and by the strength of mixing within the vortex region. In a model study of the 1994 winter and spring, *Lee* [1996] showed that during late winter, ozone loss did not propagate poleward significantly faster than the terminator. This result suggested that the mixing of air between the vortex-edge region and the vortex core was weak, but the study did not assess the accuracy of this aspect of the model.

Similar results were found in a model study of the 1996 winter and spring [*Lee et al.*, 2000], using the same model as in this work (see section 4). Measurements of ozone were also assessed and showed very good agreement with all aspects of the model calculations.

[1]Centre for Atmospheric Science, Department of Chemistry, University of Cambridge, Cambridge, England.

[2]British Antarctic Survey, Cambridge, England.

[3]Centre for Atmospheric Science, Department of Applied Mathematics and Theoretical Physics, Cambridge, England.

[4]Department of Meteorology, University of Edinburgh, Edinburgh, Scotland.

Paper number 2000JD900398.
0148-0227/01/2000JD900398$09.00

However, these studies could not differentiate whether this mixing property was a result of either the whole vortex, or just the region near the vortex edge, being a region of weak mixing. Nor could they tell if the region near the vortex edge remained isolated from the vortex core after late winter, as this cannot easily be determined from models or measurements of ozone because of the nature of the latitudinal gradients in ozone.

In spring, there are frequent instances of large planetary waves which distort the vortex such that its edge region is over populated areas of southern South America [*Jones et al.*, 1998]. During one such episode at Punta Arenas (53°S) in 1995, the ozone column fell from more than 310 Dobson units (DU) on October 8 to 200 DU on October 13 [*Kirchhoff et al.*, 1997]. If such low-ozone events happen late enough in spring when the midday Sun is at higher elevation, the lack of ozone can cause significant increases in UVB radiation with the potential for biological damage [*Lubin and Jensen*, 1995].

In this paper, we diagnose the transport structure of the lower stratosphere, enabling us to investigate the isolation of the vortex-edge region from the vortex core. The impact this isolation has on the development of the Antarctic ozone hole is investigated using a three-dimensional chemical transport model.

In our results, we avoid zonal averages at fixed latitudes because reversible dynamical effects such as fluctuations in the shape of the vortex can be wrongly attributed to mixing. Instead, we use a tracer-based equivalent-latitude coordinate (the equivalent latitude is the latitude at which a tracer contour would lie if the tracer distribution was deformed into a zonally symmetric atmosphere while conserving the area within tracer contours, a technique first used by *Butchart and Remsberg* [1986]). Calculation is based on an advected artificial tracer initialized with potential vorticity (PV [*Hoskins et al.*, 1986]) before the period of study, rather than the noisier PV calculated directly from the meteorological analyses. This artificial tracer is used as the basis for all the equivalent latitude calculations in this study. It should also be noted that this artificial tracer is also used for diagnostic studies of transport and mixing in section 2.

2. Diagnosing the Flow Structure in the Lower Stratosphere

The isolation of the polar vortex from the surf zone in the middle latitudes is due in part to the Rossby-restoring mechanism in the large scale, and in part to horizontal wind shear acting at smaller scales [*Juckes and McIntyre*, 1987]. The importance of the vortex-edge region as a barrier to transport has motivated many studies of atmospheric transport [e.g., *Norton*, 1994; *Waugh et al.*, 1994; *Chen*, 1994]. It is useful to note that the equatorward limit of the vortex-edge region represents the "vortex boundary," delineating the vortex from the surf zone.

However, few studies have examined mixing between the vortex-edge region and the vortex core. *Paparella et al.* [1997] found significant apparent mixing when the vortex-edge region was defined by PV gradients, but when they used a new vortex definition based on kinetic energy, a broad isolated region emerged in the vortex edge (their Figure 8a).

Recently, diagnostics of transport and mixing behavior calculated from tracer fields have been developed by *Nakamura* [1996] and applied to satellite observations of chemical species [*Nakamura and Ma*, 1997]. The diagnostic calculated is the equivalent length (L_{eq}), which is a measure of the geometric structure of the tracer and hence of the mixing strength. Regions of strong mixing have large values of equivalent length and regions of weak mixing (those associated with barriers to transport) have small values.

In our study, following *Haynes and Shuckburgh* [2000], the equivalent length is calculated from an artificial tracer field advected on isentropic surfaces. The tracer field was initialized on May 1, 1996, with the potential vorticity distribution and advected using U. K. meteorological analyses at 1° latitude × 1° longitude resolution.

For presentation purposes the square of the equivalent length is normalized by the square of the circumference of the zonal circle at the equivalent latitude of the tracer contour to give the quantity Λ_{eq} defined by

$$\Lambda_{eq}(\phi_e, t) = \frac{L_{eq}^2}{(2\pi r \cos\phi_e)^2} = \frac{r^2}{(\partial/\partial\phi_e)^2} \frac{\oint |\nabla c|^2 \frac{dl}{|\nabla c|}}{\oint \frac{dl}{|\nabla c|}}. \quad (1)$$

Here ϕ_e is the equivalent latitude, r is the radius of the Earth, and the integrals are around a tracer contour $c(x, y, t) = C$. For further details and discussion, see *Shuckburgh et al.* [2000].

Figure 1 shows the evolution of the lognormalized equivalent length as a function of equivalent latitude on the 480 K isentropic surface during the 1996 winter and spring. The region of strongest mixing is associated with the surf zone in the middle latitudes [*Juckes and McIntyre*, 1987]. During the winter a broad region of weak mixing between equivalent latitudes of 58°S and 68°S (the vortex-edge region) separates regions of comparatively strong mixing in the middle latitudes and the vortex core. Air masses within this vortex-edge region of weak mixing will remain isolated from either the middle latitudes or the vortex core. It is appropriate to identify the equatorward limit of this region of weak mixing with the vortex boundary. Thus within the polar vortex there are two distinct regions of approximately equal area identified by their mixing characteristics. As spring progresses, the region of weak mixing persists, but its width and position change over the season. After mid-October the region starts to narrow

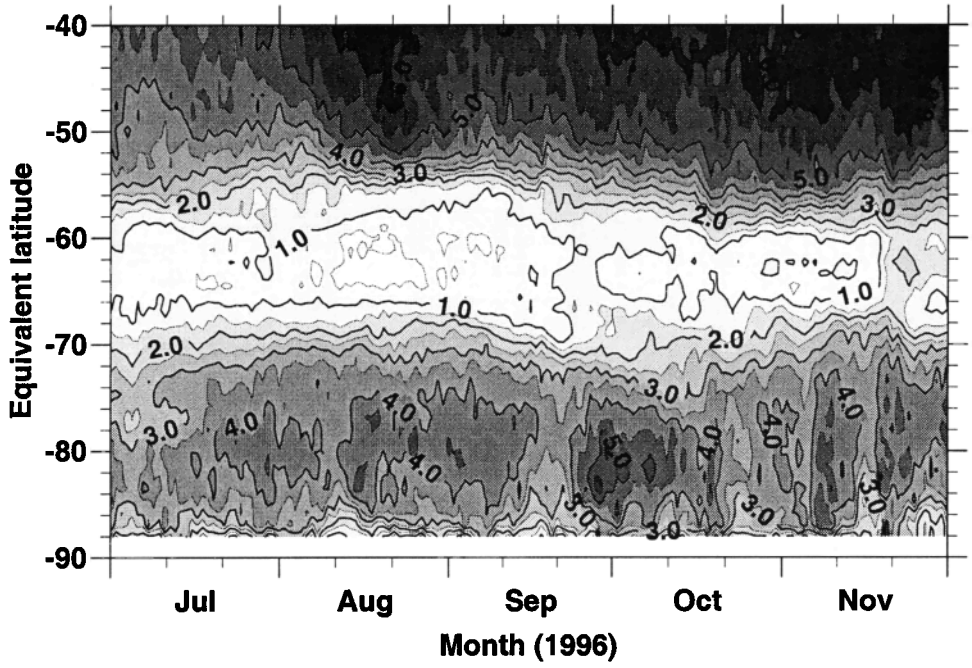

Figure 1. The evolution of lognormalized equivalent length as a function of equivalent latitude on the 480 K isentropic surface during the 1996 winter and spring. The broad region of weak mixing centered at around 63°S equivalent latitude will act as a significant transport barrier preventing the mixing of air in the vortex core with air in the middle latitudes.

and in late November there is an increase in equivalent length in the region, indicating that in late November the ability of this region to act as a barrier to transport has been reduced. Note that *Haynes and Shuckburgh* [2000] only found evidence of mixing in the vortex core in the midstratosphere. This is believed to be a consequence of the lower resolution used in the tracer calculations of that study.

Equivalent length is a function of equivalent latitude and hence of tracer concentration. It may therefore be regarded, just as a tracer concentration may be regarded, as a function of latitude and longitude. Thus isentropic distributions of equivalent length can be achieved by mapping the equivalent length onto the isentropic distribution of equivalent latitude. Figure 2 shows the lognormalized equivalent length for September 1, 1996, on the 480 K isentropic surface. In this representation it is strikingly clear how a broad ring of weak mixing (the vortex-edge region) separates two regions of comparatively strong mixing in the middle latitudes and in the vortex core.

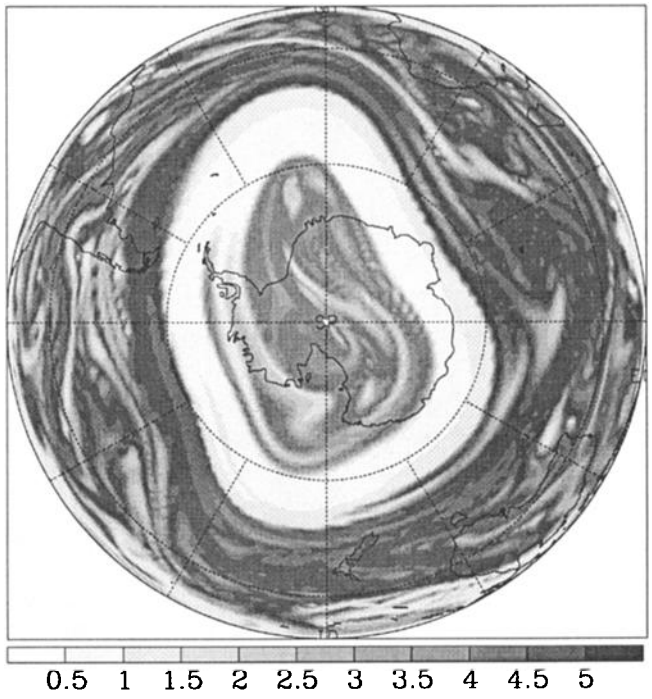

Figure 2. Lognormalized equivalent length for September 1, 1996 mapped onto the 480 K isentropic surface using the equivalent latitude distribution. The region of weak mixing identified in Figure 1 is distributed as a broad ring separating regions of comparatively stronger mixing in the vortex core and the middle latitudes.

3. Weak Mixing Inferred From Measurements of Water Vapor in the Vortex-Edge Region

The calculations of section 2 relied on the accuracy of meteorological analyses in a data-poor area, so we examined measurements of tracers which might help di-

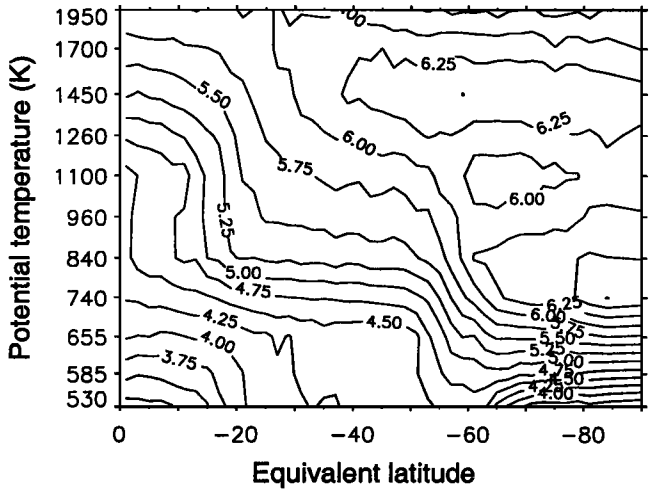

Figure 3. Equivalent latitude-potential temperature cross section of water vapor measured by MLS from August 19 to 23, 1992 (taken from *Morrey* [1997]). Oxidation of CH_4 creates moist air aloft, which descends during poleward transport in winter. The low temperatures in the lower stratospheric vortex core form PSC ice particles which are large enough to sediment, leading to dehydration. Following dehydration, a water vapor maximum appears in the vortex-edge region.

agnose mixing. In Antarctica, water vapor is a particularly useful tracer. Descent throughout the vortex during winter brings air from aloft, which following methane oxidation is rich in water vapor. Microwave Limb Sounder (MLS [*Waters,* 1993]) water vapor measurements in Figure 3 show this behavior very clearly. The low temperatures in the vortex core form PSC ice particles which are large enough to sediment, leading to dehydration, as can also be inferred from Figure 3. In the lower stratosphere, it leads to a dry vortex core surrounded by a ring of more humid air in the vortex-edge region, with drier air outside the ring at middle latitudes. Persistence of this pattern after dehydration has ceased in September would suggest isolation of the vortex core from the vortex-edge region.

Water vapor from the MLS instrument aboard the Upper Atmosphere Research Satellite (UARS) is now retrieved with a nonlinear algorithm which extends the retrieval into optically thicker regions at lower altitudes [*Pumphrey,* 1999]. Figure 4 shows the evolution of MLS water vapor as a function of equivalent latitude on the 480 K isentropic surface during the 1992 spring. The expected pattern is seen throughout September. During October the MLS instrument is pointing northward. When in November the instrument is again pointing southward a drier vortex core is still visible, although some moistening has occurred. More complete mixing between vortex core and edge occurs during November, before the final vortex breakdown.

4. Chemical Model Calculations for 1996

In this section we present calculations from a three-dimensional chemical transport model SLIMCAT. The model, described by *Chipperfield et al.* [1996], is for-

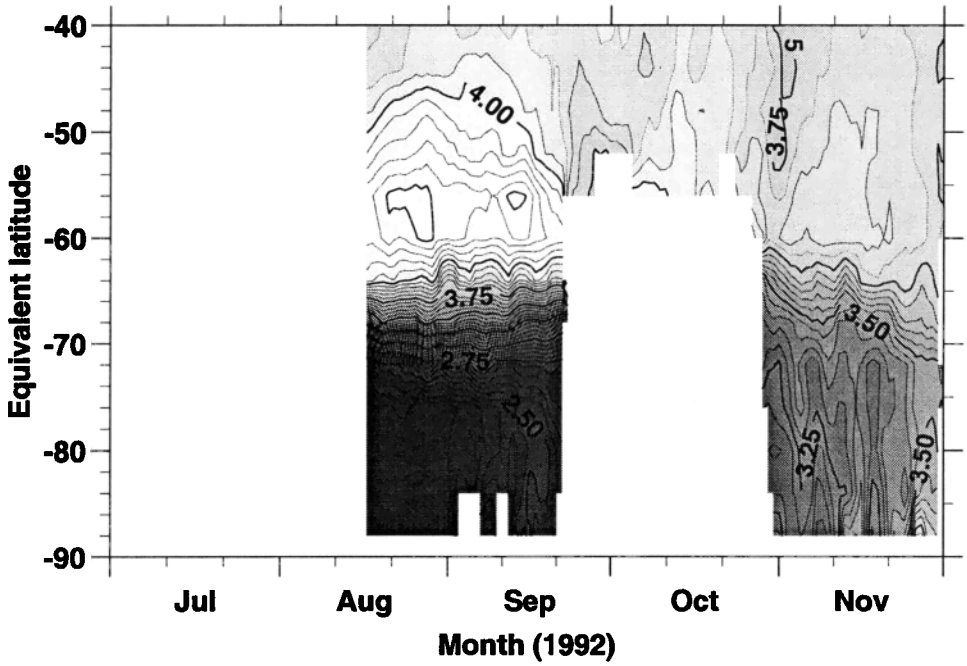

Figure 4. The evolution of MLS water vapor as a function of equivalent latitude on the 480 K isentropic surface during the 1992 spring. The water vapor was averaged within 4° equivalent latitude bands. The MLS measurements show the contrast in water vapor between the vortex-edge region and the drier vortex core during spring. This supports our analysis of weak mixing diagnosed by equivalent length (Figure 1).

mulated in an isentropic coordinate. The upstream advection scheme is based on conservation of second-order moments of tracer distribution during advection [*Prather*, 1986]. The circulation and temperatures are specified from the 24-hourly analyses of the U.K. Meteorological Office data assimilation system [*Swinbank and O'Neill*, 1994]. Vertical motion is derived from heating rates calculated by the radiation scheme of *Shine* [1987]. The transport code is coupled to a detailed stratospheric chemistry scheme, including heterogeneous reactions.

The model was initialized from a low-resolution multiannual simulation, details of which have been reported by *Chipperfield* [1999]. The model simulation was started on May 9, 1996, and continued until November 15, 1996. The resolution was 2.5° latitude and 5.6° longitude. There were 12 isentropic levels in the vertical, at intervals of between 1.5 and 2.0 km in the lower stratosphere. General model accuracy was confirmed by comparing the model ozone field with numerous ozonesondes [*Lee et al.*, 2000], showing very good agreement.

The ozone tendencies associated with catalytic ozone loss cycles are easily diagnosed within the model. The dominant ozone loss cycle in the polar region is the ClO dimer cycle [*Molina and Molina*, 1987]:

$$\begin{aligned} \mathrm{ClO} + \mathrm{ClO} + \mathrm{M} &\longrightarrow \mathrm{Cl_2O_2} + \mathrm{M} \\ \mathrm{Cl_2O_2} + h\nu &\longrightarrow \mathrm{Cl} + \mathrm{ClOO} \\ \mathrm{ClOO} + \mathrm{M} &\longrightarrow \mathrm{Cl} + \mathrm{O_2} + \mathrm{M} \\ 2 \times (\mathrm{Cl} + \mathrm{O_3} &\longrightarrow \mathrm{ClO} + \mathrm{O_2}) \\ \text{net: } \mathrm{O_3} + \mathrm{O_3} &\longrightarrow \mathrm{O_2} + \mathrm{O_2} + \mathrm{O_2}. \end{aligned}$$

In the middle latitudes, where ClO concentrations are a small fraction of those found in the wintertime polar vortex, the rate of the ClO dimer cycle is insignificant. Thus air masses which have experienced ozone loss due to this cycle are air masses of polar vortex origin. Figure 5 shows the evolution of ozone loss (ppmv) due to the ClO dimer cycle as a function of equivalent latitude on the 480 K isentropic surface: loss begins in midwinter at the vortex edge where it protrudes out of polar night, as confirmed by observations [*Roscoe et al.*, 1997]; loss remains confined to the sunlit side of the terminator until the end of July; subsequently, ozone loss rapidly penetrates the region poleward of the terminator [*Lee et al.*, 2000].

However, a maximum in ozone loss persists in the vortex-edge region until mid-September. This is readily interpreted in terms of the equivalent length. Ozone loss which occurs within the region of weak mixing remains largely confined to that region, and ozone loss which

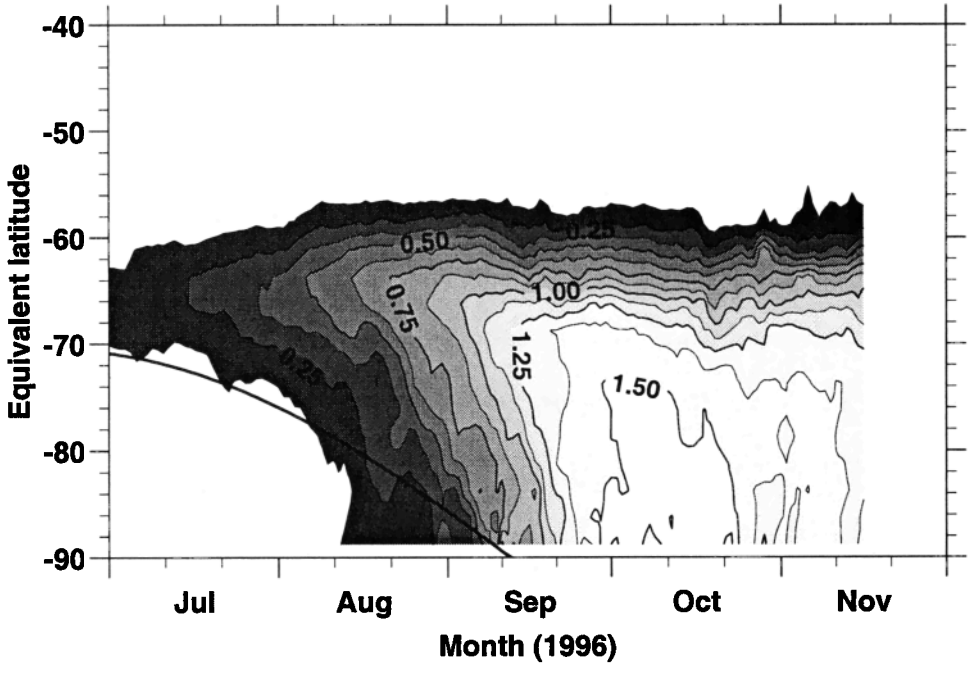

Figure 5. The evolution of accumulated model ozone loss due to the ClO dimer cycle as a function of equivalent latitude on the 480 K isentropic surface (reproduced from *Lee et al.* [2000]). The ozone loss has been averaged within 2.5° equivalent latitude bands. Contours of ozone loss are given in mixing ratios (ppmv). The bold line shows the approximate latitudinal position of the terminator on the 480 K isentropic surface. During winter and early spring, significant ozone loss is strongly confined to the sunlit region at the edge of the vortex.

occurs in the region of strong mixing within the vortex core is rapidly mixed throughout the vortex core. In the vortex-edge region, stratospheric temperatures are generally warmer than in the core [e.g., *Tao & Tuck*, 1994], so that PSCs are less frequent and so there is less reactive chlorine. However, the edge region sees more sunlight earlier in the year. This combination results in greater ozone loss in the edge region until mid-September. It should be noted that all the ozone loss shown in Figure 5 occurs and remains confined to the polar vortex.

Further, we can determine the confinement of ozone loss occurring within the vortex-edge region. Although the edge region occupies a broad band of width 10° in equivalent latitude, one problem is that its mean equivalent latitude changes during the winter and spring. However, Figure 1 shows that the 60° to 65°S equivalent-latitude range remains a region of weak mixing throughout the winter and spring. Hence we can explore the confinement by examining ozone loss which occurs only within this narrower range and by following that ozone loss as it is transported to other equivalent latitudes. This was done during the model run by calculating a tracer which is the integral only of ozone loss that occurs in a particular equivalent latitude band. The tracer is then advected by the analyzed winds in the same way as other trace gases in the model: no specific trajectories need be calculated.

Figure 6 shows the evolution of ozone loss which occurs in the equivalent latitude range 60° to 65°S: the loss remains confined to the vortex edge region until mid-October. To determine how this compares to the evolution of ozone loss which occurs within the vortex core, Figure 7 shows the evolution of ozone loss which occurs in the equivalent latitude range 70° to 75°S: the loss is rapidly mixed throughout the core, rather than being confined to the equivalent-latitude band at which the loss originally occurred.

5. Discussion

From our modeling studies we now have a new picture of the Antarctic ozone hole. There are two regions which remain distinct until at least mid-October: a core which is well mixed and a broad edge region in which mixing is weak. The properties of each region differ considerably. In the edge region, stratospheric temperatures are warmer and so PSCs are less frequent, but it sees more sunlight earlier in the year. This results in greater ozone loss in the edge region until mid-September (Figure 5).

Although the area covered by the two regions is similar, the fact that isentropic surfaces bend upward to lower pressures at the pole means that the edge region is more massive than the core. As a result, by the end of September, approximately 20% more ozone loss occurs

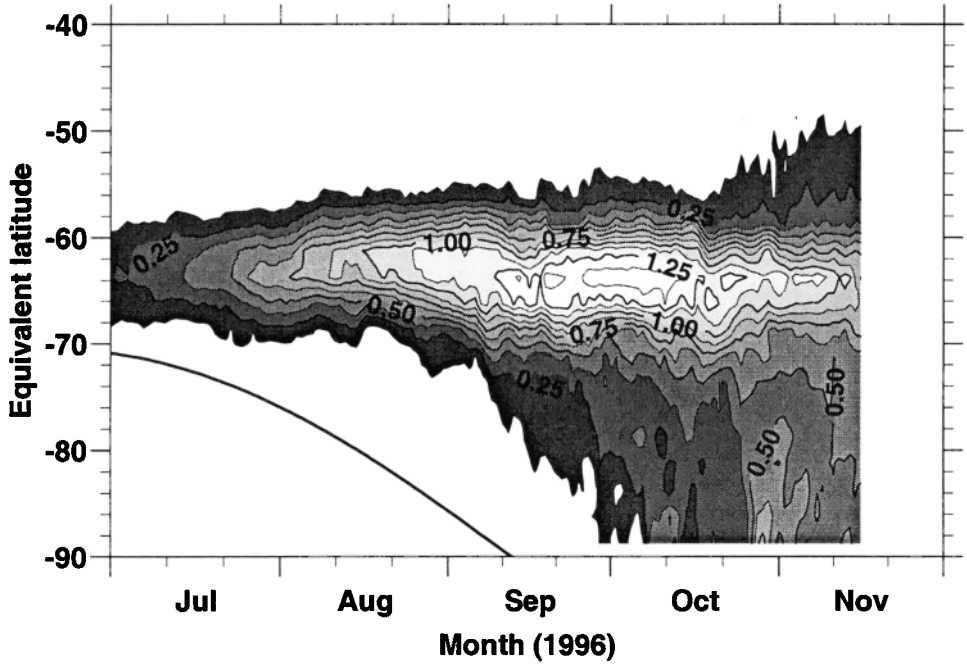

Figure 6. The evolution of accumulated model ozone loss that occurred within the 60° to 65°S equivalent latitude band as a function of equivalent latitude on the 480 K isentropic surface. The ozone loss has been averaged within 2.5° equivalent latitude bands. Contours of ozone loss are labeled as mixing ratios (ppmv). The bold line shows the approximate latitudinal position of the terminator on the 480 K isentropic surface. The ozone loss remains largely confined to the region of weak mixing until at least mid-spring.

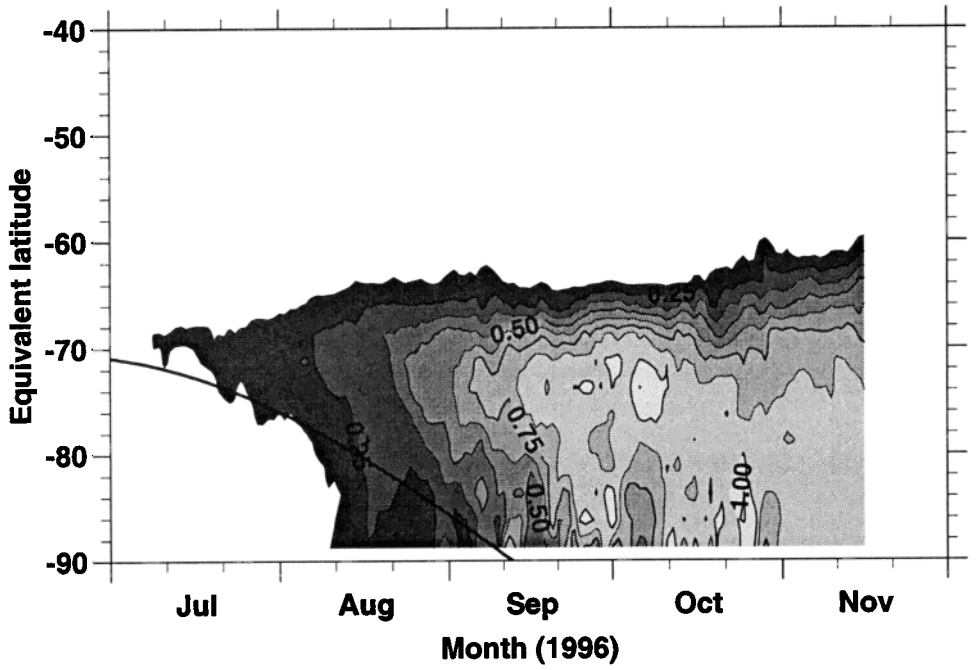

Figure 7. As Figure 6, but for ozone loss that occurred within the 70° to 75°S equivalent latitude band. Transport of ozone loss southward soon after it occurs at these latitudes in early spring (August) is clearly evident, unlike Figure 6. This illustrates the comparatively well-mixed nature of the vortex core.

within the 60° to 70°S equivalent-latitude band than occurs further poleward: the edge region is not the minor part of the ozone hole that might be thought from linear latitudinal plots.

Because of the lack of mixing, the properties of the edge region contribute separately to the ozone loss potential averaged over the Antarctic as a whole. Together with the larger mass of the edge region, this clearly has implications for the ozone deficit averaged over the whole Southern Hemisphere after vortex breakdown. These implications are beyond the scope of this paper.

This new picture of the ozone hole also has implications for future ozone loss. Ozone loss in the edge region is limited by a function both of PSC amount and of the supply of unreactive chlorine, unlike ozone loss in the vortex core where PSCs are ubiquitous.

PSC amounts are determined by the temperature of the lower and middle stratosphere, whose global average has cooled by about 1 K since 1980 [e.g., *Pyle et al.*, 1999]. Calculations by *Forster and Shine* [1999] indicate that this cooling has arisen from observed increases in CO_2 and H_2O and reductions in ozone. We do not understand the causes of the increases in H_2O [*Pyle et al.*, 1999], and cooling by reduced ozone acts as a positive feedback which causes significant uncertainty about its future size. However, CO_2 is expected to continue to increase during the next 50 years.

If current trends continue, a likely result will be an increased frequency of PSCs in the Antarctic vortex-

Table 1. Ratios to That in the Control Run of Ozone Loss Calculated by Model Runs With Different Amounts of Total Chlorine and Different Temperatures.

	Total Cl, ppbv							
	ClO-Dimer Cycle				All Cycles			
ΔT, K	3.6	3.0	2.5	2.0	3.6	3.0	2.5	2.0
0	1.00	0.79	0.61	0.44	1.00	0.92	0.83	0.72
-2	1.12	0.91	0.72	0.53	1.09	1.02	0.93	0.82
-4	1.21	1.00	0.80	0.60	1.15	1.09	1.00	0.89
-6	1.28	1.07	0.87	0.66	1.18	1.13	1.05	0.94
-8	1.34	1.13	0.93	0.71	1.20	1.15	1.08	0.96

The ozone loss was averaged over the equivalent latitude band from 60° to 65°S on October 16, 1996, on the 480 K isentropic surface. Loss due to the catalytic cycle involving the ClO dimer and net loss due to all cycles were independently diagnosed.

edge region during the mid-21st century, similar to that predicted in the Arctic vortex as a whole [*Shindell et al.*, 1998]. In the edge region of the Antarctic vortex, the result will be a more complete conversion of unreactive chlorine into reactive forms and thus more ozone loss than otherwise.

To test this theory, the model was run at different temperatures and different amounts of total chlorine loading (i.e., both inorganic and organic chlorine). Values of net ozone loss in spring in the isolated vortex-edge region, both from the ClO dimer cycle and from all cycles, are listed in Table 1. The table shows that if temperatures were 4 K colder, ozone loss similar to or greater than today's values would occur at all total chlorine loadings greater than 2.5 ppbv. The chlorine loading of the atmosphere is forecast to remain greater than 2.5 ppbv until after 2030 [*Pyle et al.*, 1999]. These results indicate that the horizontal extent of the ozone hole, which depends on the ozone loss in the weakly mixed vortex-edge region will not recede until after 2030 if this region cools by 4 K or more.

Hence as the amounts of halocarbons decline according to the provisions made in the Montreal Protocol, we would not expect ozone depletion in the vortex-edge region to recover as rapidly as anticipated for the vortex core. It is ozone-depleted air in the isolated vortex-edge region that frequently passes over populated areas of southern South America, where in mid-October the midday Sun is at sufficiently high elevation for significant UV damage to occur during low column ozone episodes.

Nor would we expect the loss averaged over the whole ozone hole to recover as rapidly as anticipated. This has obvious implications for future ozone values in late summer in the Southern Hemisphere as a whole.

Acknowledgments. We thank M. P. Chipperfield and J. A. Pyle for SLIMCAT code, and S. J. Oltmans and R. S. Harwood for useful discussions. A. M. Lee thanks UGAMP and DETR EPG 1/1/83 for funding. P. H. Haynes thanks UGAMP and EC (TOASTE-C). E. F. Shuckburgh thanks NERC, EC through the Polar Vortex Change project (ENV4-CT97-0540) and Trinity College, Cambridge. M. W. Morrey and H. C. Pumphrey thank NERC for funding. The Centre for Atmospheric Science is a joint initiative of the Department of Applied Mathematics and Theoretical Physics and the Department of Chemistry at the University of Cambridge.

References

Butchart, N., and E. E. Remsberg, The area of the stratospheric polar vortex as a diagnostic for tracer transport on an isentropic surface, *J. Atmos. Sci., 43*, 1319–1339, 1986.

Cacciani, M., G. Fiocco, P. Colagrande, P. Di Girolamo, A. di Sarra, and D. Fua, Lidar observations of polar stratospheric clouds at the South Pole, 1, Stratospheric unperturbed conditions, *J. Geophys. Res., 102*, 12,937–12,943, 1997.

Chen, P., The permeability of the Antarctic vortex edge, *J. Geophys. Res., 99*, 20,563–20,571, 1994.

Chipperfield, M. P., Multiannual simulations with a three-dimensional chemical transport model, *J. Geophys. Res., 104*, 1781–1805, 1999.

Chipperfield, M. P., M. L. Santee, L. Froidevaux, G. L. Manney, W. G. Read, J. W. Waters, A. E. Roche, and J. M. Russell, Analysis of UARS data in the southern polar vortex in September 1992 using a chemical transport model, *J. Geophys. Res., 101*, 18,861–18,881, 1996.

Dunkerton, T. J., C.-P. Hsu, and M. E. McIntyre, Some Eulerian and Lagrangian diagnostics for a model stratospheric warming, *J. Atmos. Sci., 38*, 819–843, 1981.

Farman, J. C., B. G. Gardiner, and J. D. Shanklin, Large losses of total ozone in Antarctica reveal seasonal ClO_x/NO_x interaction, *Nature, 315*, 207–210, 1985.

Forster, P. M. de F., and K. P. Shine, Stratospheric water vapor changes as a possible contributor to observed stratospheric cooling, *Geophys. Res. Lett., 26*, 3309–3312, 1999.

Haynes, P. H., and E. F. Shuckburgh, Effective diffusivity as a diagnostic of atmospheric transport, 1, Stratosphere, *J. Geophys. Res., 105*, 22,777–22,794, 2000.

Hoskins, B. J., M. E. McIntyre, and A. W. Robertson, On the use and significance of isentropic potential vorticity maps, *Q. J. R. Meteorol. Soc., 111*, 877–946, 1986. (Corrigendum, *Q. J. R. Meteorol. Soc., 113*, 402–404, 1986.)

Jones, A. E., T. Bowden, and J. Turner, Predicting total ozone based on GTS data: Applications for South American high-latitude populations, *J. Appl. Meteorol., 37*, 477–485, 1998.

Juckes, M. N., and M. E. McIntyre, A high-resolution, one-layer model of breaking planetary waves in the stratosphere, *Nature, 328*, 590–596, 1987.

Kirchhoff, V. W. J. H., C. A. R. Casiccia, and F. Zamorano, The ozone hole over Punta Arenas, Chile, *J. Geophys. Res., 102*, 8945–8953, 1997.

Lee, A. M., Numerical modelling of stratospheric ozone, Ph.D. thesis, Univ. of Cambridge, Cambridge, England, 1996.

Lee, A. M., H. K. Roscoe, and S. Oltmans, Model and measurements show Antarctic ozone loss follows edge of polar night, *Geophys. Res. Lett., 27*, 2000.

Lubin, D., and E. H. Jensen, Effects of clouds and stratospheric ozone depletion on ultra-violet radiation trends, *Nature, 377*, 710–713, 1995.

McCormick, M. P., Aerosol measurements from Earth orbiting spacecraft, *Adv. Space Res., 2*, 73–86, 1983.

Molina, L. T., and M. J. Molina, Production of Cl_2O_2 from the self-reaction of the ClO radical, *J. Phys. Chem., 91*, 433–439, 1987.

Morrey, M. W., Observations of barriers to mixing in the stratosphere, Ph.D. thesis, Univ. of Edinburgh, Edinburgh, Scotland, 1997.

Nakamura, N., Two-dimensional mixing, edge formation, and permeability diagnosed in an area coordinate, *J. Atmos. Sci., 53*, 1524–1573, 1996.

Nakamura, N., and J. Ma, Modified Lagrangian-mean diagnostics of the stratospheric polar vortices, 2, Nitrous oxide and seasonal barrier migration in the cryogenic limb array etalon spectrometer and SKYHI general circulation model, *J. Geophys. Res., 102*, 25,721–25,735, 1997.

Norton, W. A., Breaking Rossby waves in a model stratosphere diagnosed by a vortex-following coordinate system and a technique for advecting material contours, *J. Atmos. Sci., 51*, 654–673, 1994.

Paparella, F., A. Babiano, C. Basdevant, A. Provenzale, and P. Tanga, A Lagrangian study of the Antarctic polar vortex, *J. Geophys. Res., 102*, 6765–6773, 1997.

Prather, M. J., Numerical advection by conservation of second-order moments, *J. Geophys. Res., 91*, 6671–6681, 1986.

Pumphrey, H. C., Validation of a new prototype water vapor retrieval for UARS MLS, *J. Geophys. Res., 104*, 9399–9412, 1999.

Pyle, J. A., et al., Stratospheric Ozone 1996, in *Report of the UK Stratospheric Ozone Review Group, DOE Ref. 96DPL0021*, DOE, London, 1996.

Pyle, J. A., et al., Stratospheric Ozone 1999, in *Report of the UK Stratospheric Ozone Review Group, DETR Ref. 99EP0458*, DETR, London, 1999.

Roscoe, H. K., A. E. Jones, and A. M. Lee, Midwinter start to Antarctic ozone depletion: evidence from observations and models, *Science, 278*, 93–96, 1997.

Shindell, D. T., D. Rind, and P. Lonergan, Increased polar stratospheric ozone losses and delayed eventual recovery owing to increased greenhouse gas concentrations, *Nature, 392*, 589–592, 1998.

Shine, K. P., The middle atmosphere in the absence of dynamical heat fluxes, *Q. J. R. Meteorol. Soc., 113*, 603–633, 1987.

Shuckburgh, E. F., W. A. Norton, A. M. Iwi and P. H. Haynes, The influence of the quasi-biennial oscillation on isentropic transport and mixing in the tropics and subtropics, *J. Geophys. Res.*, in press, 2000.

Swinbank, R., and A. O'Neill, A stratosphere-troposphere data assimilation system, *Mon. Weather Rev., 122*, 686–702, 1994.

Tao, X., and A. F. Tuck, On the distribution of cold-air near the vortex edge in the lower stratosphere, *J. Geophys Res., 99*, 3431–3450, 1994.

Waters, J. W., *Atmospheric Sensing by Microwave Radiometry*, edited by M. A. Janssen, John Wiley, New York, 1993.

Waugh, D. W., et al., Transport out of the lower stratospheric Arctic vortex by Rossby wave breaking, *J. Geophys. Res., 99*, 1071–1088, 1994.

World Meteorological Organization, Scientific assessment of stratospheric ozone: 1989, in *Global Ozone Research and Monitoring Project, Rep. 20*, edited by D. L. Albritton and R. T. Watson, p.viii, Geneva, 1989.

P. H. Haynes and E. F. Shuckburgh, Centre for Atmospheric Science, Department of Applied Mathematics and Theoretical Physics, University of Cambridge, Silver Street, Cambridge, England CB3 9EW. (email: P.H.Haynes@damtp.cam.ac.uk)

A. E. Jones and H. K. Roscoe, British Antarctic Survey/NERC, Madingley Road, Cambridge, England CB3 0ET. (e-mail: h.roscoe@bas.ac.uk)

A. M. Lee, Centre for Atmospheric Science, Department of Chemistry, University of Cambridge, Lensfield Road, Cambridge, England CB2 1EW. (e-mail: Adrian.Lee@atm.ch.cam.ac.uk)

M. W. Morrey and H. C. Pumphrey, Department of Meteorology, University of Edinburgh, Kings Buildings, Mayfield Road, Edinburgh, Scotland EH9 3JZ. (email: H.C.Pumphrey@met.ed.ac.uk)

(Received April 7, 2000; revised June 22, 2000;
accepted June 29, 2000.)